ChemComm

COMMUNICATION

View Article Online
View Journal | View Issue

Cite this: *Chem. Commun.*, 2014, **50**, 8747

Received 23rd April 2014,
Accepted 10th June 2014

DOI: 10.1039/c4cc03024a

www.rsc.org/chemcomm

Conjugates of tetraphenylethene and diketopyrrolopyrrole: tuning the emission properties with phenyl bridges†

Xiao Yuan Shen,‡[a] Yi Jia Wang,‡[a] Haoke Zhang,[a] Anjun Qin,[ab] Jing Zhi Sun*[a] and Ben Zhong Tang*[abc]

Diketopyrrolopyrrole (ACQ-gen) and tetraphenylethenes (AIE-gen) are linked together with phenyl bridges. The derivatives show substantially enhanced and red-shifted emission in the solid state.

Great efforts have been devoted to the development of high-performance organic luminogens that can be used in organic light-emitting diodes (OLEDs), bio- and chemo-sensors.[1] For a long time, it has been noted that lots of organic luminogenic molecules suffer from the "aggregation-caused quenching" (ACQ) effect. That is, their aggregates or solids show drastic emission quenching due to the adverse intermolecular interactions.[2] This has seriously restricted their application in the solid state. The discovery of "aggregation-induced emission" (AIE) opens an avenue to improving the fluorescence quantum yield of organic molecules in aggregated/solid states.[3] AIE active molecules thus have attracted considerable attention in the fields of OLEDs, mechanochromic materials and bioimaging.[4]

Tetraphenylethene (TPE) and its derivatives are representatives of AIE active molecules, which possess prominent AIE properties and enjoy the easiness to be synthesized.[5] TPE is also used as an AIE-generator (AIE-gen) to modify traditional luminogens such as triphenylamine, pyrene, and perylenebisimide and successfully converted them from ACQ to AIE molecules.[6] Diketopyrrolopyrrole (DPP) is another classical luminogen. DPP and its derivatives emit strong fluorescence in dilute solution and show excellent thermal and photo-stability. They play an active role in photovoltaic cells, field-effect transistors and fluorescent probes.[7] As a consequence of the well-conjugated DPP core, however, they display a typical ACQ effect. Thus, it is of significance to examine the availability of tuning the emission performance of DPP by rational modifications.

The strategy used here is to modify the DPP core by linking two TPE moieties at its α-positions directly (DTPE–DPP, **1**) and indirectly (DTPE-Dph-DPP, **2**) *via* phenyl groups. Considering that DPP is a typical electron acceptor, we also designed and synthesized other DPP derivatives, which were further modified with electron donors (D), *i.e. N*,*N*-dimethylamine groups on different phenyls of the TPE moieties (molecule **3** and its isomer **4**).

The molecular structures of **1** to **4** are shown in Chart 1 and their synthetic routes are shown in Schemes S1 to S5 in the ESI.†

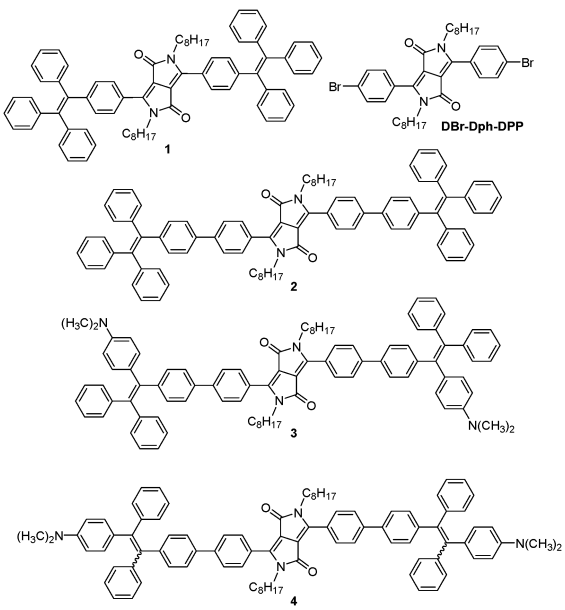

Chart 1 Molecular structures of the TPE–DPP conjugates.

[a] *MOE Key Laboratory of Macromolecule Synthesis and Functionalization, Department of Polymer Science and Engineering, Zhejiang University, Hangzhou 310027, China. E-mail: sunjz@zju.edu.cn*

[b] *Guangdong Innovative Research Team, State Key Laboratory of Luminescent Materials and Devices, South China University of Technology, Guangzhou 510640, China*

[c] *Department of Chemistry, Institute for Advanced Study, Institute of Molecular Functional Materials, and State Key Laboratory of Molecular Neuroscience, The Hong Kong University of Science and Technology, Clear Water Bay, Kowloon, Hong Kong, China. E-mail: tangbenz@ust.hk*

† Electronic supplementary information (ESI) available: Synthetic details; ^{1}H NMR and ^{13}C NMR spectra, mass spectra, CV curves, UV-visible and PL spectra, and thermal gravimetric curves of the molecules; SEM and confocal FL images of the molecular aggregates. See DOI: 10.1039/c4cc03024a

‡ X. Y. Shen and Y. J. Wang contributed equally to this work.

Also shown in Chart 1 is the molecular structure of the intermediate DBr-Dph-DPP, which is a crucial intermediate and used for property comparison with its derivatives. The experimental details and the data of the structure characterization are provided in ESI.† The purity of the resultants and intermediates has been confirmed by elemental analysis, ^{1}H NMR, ^{13}C NMR and high resolution mass spectroscopic techniques (Fig. S1 to S8, ESI†). Due to the *N*-term modified octyl chain, all of them have good solubility in common organic solvents. This allows their electronic structures to be evaluated with optical absorption, fluorescent emission and cyclic voltammetry (CV) measurements in solution.

The results of CV measurements demonstrate that all of these DPP derivatives have a pair of redox waves under negative bias (Fig. S9, ESI†), suggesting that the electron acceptor character of the DPP core remains unchanged after the chemical modifications. Thermo-gravimetric analysis results indicate that the decomposition point for molecules DBr-DPh-DPP, **1**, **2**, and **3** is 318, 389, 419 and 407 °C, respectively (Fig. S10, ESI†). These data indicate that the TPE-modified DPP derivatives have improved thermal stability.

The property that we are most interested in is their fluorescent behaviors. As demonstrated by the spectra in Fig. 1 and Fig. S11 and the data in Table S1 (ESI†), in tetrahydrofuran (THF) solution, molecule **1** emits yellow fluorescence (λ_{em} = 572 nm) and the quantum efficiency (Φ_F) is 13.6%. When relative low fraction of water (f_w, by volume), a non-solvent to **1**, is introduced into the THF solution, the change in emission intensity is quite small. When f_w reaches 50%, the emission intensity decreases evidently. When f_w is over 70%, the emission becomes much weaker and the change in Φ_F *vs.* f_w is shown in Fig. 1B. The Φ_F is only 1.27% at f_w of 95%. The above data indicate a typical ACQ behavior and the quenching factor (Φ_q) is calculated to be 90.7% (ESI†). The decrease of Φ_F against the increase of f_w can be ascribed to the formation of aggregates in the THF–water mixtures, which quenches the fluorescence *via* the intermolecular π–π interaction. Besides the decrease in Φ_F, the emission peak red-shifted from 572 to 585 nm with the increase of f_w from 0 to 95%. The Φ_F of the solid film of **1** is 11.8%, because in this case molecule **1** locates in a low polar environment without being surrounded by high polar water molecules (Table S1, ESI†). These changes will be discussed below together with molecules **2** and **3**.

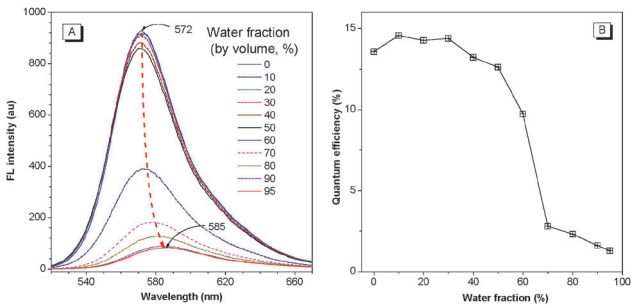

Fig. 1 Change in fluorescence (FL) intensity (A) and quantum efficiency (Φ_F) (B) of molecule **1** in THF–water mixtures with different water fractions (f_w). Concentration: 10 μM; λ_{ex}: 365 nm.

The fluorescent behaviors observed above for molecule **1** are quite different from our previous reports on TPE-modified pyrene, perylene-bisimide and triphenylamine derivatives, where the linking of TPE moieties onto these cores has converted them from ACQ to AIE active molecules (Chart S1, ESI†).[6,8] It seems that the TPE-modification has no effect on the emission behaviors of DPP. To get an understanding of this abnormal phenomenon, we carefully examined the electronic structure of molecule **1** and found that the two phenyl groups in TPEs, which are directly linked to the DPP moiety, have conjugated with DPP. In other words, they are merged into a new fluorogen. **1** should be considered as a diphenyl-DPP core (Dph-DPP) modified by two 1,2,2-triphenylethene groups but not a DPP core modified by two TPE moieties (*cf.* Chart S2 and Fig. S12, ESI†).

This is readily confirmed by examining the fluorescent behavior of DBr-Dph-DPP. As revealed by the data in Tables S1, S2 and Fig. S13 (ESI†), in dilute THF solution, DBr-Dph-DPP emits yellow-greenish fluorescence with a peak at 543 nm (λ_{em}) and the Φ_F is 95.2%. But Φ_F falls to 0.95% in the THF–water mixture at f_w of 95% and Φ_q is calculated to be 99.0%. These data indicate that DBr-Dph-DPP is a typical ACQ molecule. The red-shift of the emission of **1** relative to DBr-Dph-DPP originates from the modification of Dph-DPP with two segments of α,β,β-triphenylethene. Meanwhile, the modification results in the decrease of Φ_F from 95.2% for DBr-Dph-DPP to 13.6% for **1** (Table S2, ESI†). This is ascribed to the intramolecular rotation of the phenyl groups, which partially exhaust the energy of the excited state. On the whole, it is obvious that molecule **1** is similar to DBr-Dph-DPP for their fluorescent behaviors.

The comparative study on fluorescent behaviors of DBr-Dph-DPP and **1** suggests that the direct linking of TPE to DPP cannot convert the DPP derivative from an ACQ to an AIE active molecule and obtain a DPP-based fluorescent material with high Φ_F in the solid state. The assimilation of DPP to TPE plays a key role. It is reasonable that the insertion of a spacer between DPP and TPE moieties may break the assimilation effect. Considering that a series of excellent studies have shown experimentally and theoretically that the phenyl ring twisting plays a key role in the organic photo/electronics.[9,10] Herein the electronic communication between DPP and TPE is crucial for tuning to the photo/electronic properties of DPP with TPE, phenyl groups, a π-conjugate building block is used as the spacer. The target molecule was derived by substituting the two bromide atoms on DBr-Dph-DPP with two TPE moieties (**2**, Chart 1).

The phenyl bridge has evidently tuned the fluorescent behaviors as compared to molecule **2** to **1** and DBr-Dph-DPP. Molecule **2** emits yellow fluorescence (λ_{em} = 568 nm) with moderate efficiency (Φ_F = 43.8%) in THF solution (Fig. 2 and Fig. S13, S15, Tables S1 and S3, ESI†). The red-shift of emission relative to DBr-Dph-DPP is associated with the segmental electronic conjugation between DPP and TPE moieties, as predicted by theoretical calculation (Fig. 3). In the free state (*e.g.*, in dilute solution), the dihedral angle between the bridge and the adjacent phenyl in the TPE moiety is about 37°, suggesting the partial conjugation between the TPE and DPP moieties. In comparison with **1**, only a 4 nm difference in the

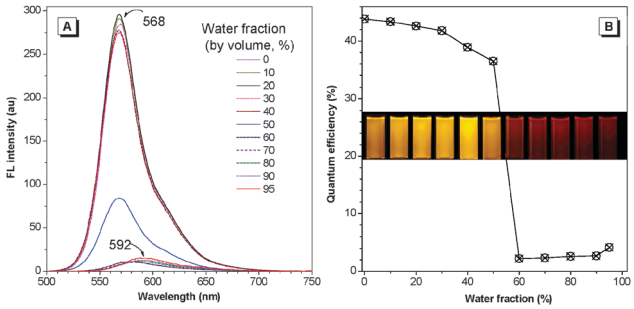

Fig. 2 Change in FL intensity (A) and Φ_F (B) of molecule **2** in THF–water mixtures with different f_w values; the inset images show the corresponding FL photographs. Concentration: 10 μM; λ_{ex}: 365 nm.

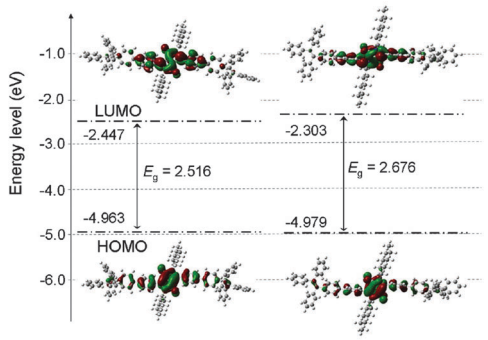

Fig. 3 Energy level alignment and electron distribution of molecule **2** with different conformations. The dihedral angles between the bridge and the adjacent phenyls in the TPE moiety are set to 15° (left) and 37° (right).

emission peak was recorded, indicating that the addition of the phenyl groups between DPP and two TPE moieties has not enlarged the effective conjugation length. Due to the steric repulsion, the phenyl bridge is not co-planar with DPP and TPE moieties (Fig. 3), thus the effects of TPE modification are abated and the properties of **2** are dominated by the DPP moiety. This is also supported by the results of CV measurement (Fig. S9, ESI†).

The Φ_F values for **2** are different from **1** and DBr-Dph-DPP in both THF solutions and solid films. The Φ_F change is ascribed to the intramolecular rotations, which can exhaust the energy of the excited state. For DBr-Dph-DPP, there are no extra rotational phenyls around the Dph-DPP core, it has the highest Φ_F (95.2%). For **1**, the rotational phenyls are closely linked to the Dph-DPP core, its Φ_F steeply decreases to 13.6%. For **2**, the linkage between the Dph-DPP core and the rotational phenyls is separated by the phenyl bridge, and rotation-caused energy dissipation is inefficient. Thus, its Φ_F is 43.8%, more than 3 times higher than that of molecule **1**. More importantly, the insertion of phenyl bridges between DPP and TPE moieties disturbs the intermolecular π–π interaction in the solid state, the Φ_F of **2** in cast films increases to 30.2%, the highest one among all molecules (Fig. S14, Tables S3 and S5, ESI†).

In THF–water mixtures, Φ_F of **2** decreases to 36.5% when f_w is 50%; whereas $f_w \geq 60\%$, the emission is heavily quenched and the Φ_F drops to 2.2%. In the solvent mixture with 95% of water, the Φ_F rises to 4.1%. Meanwhile, the emission peak shifts to 592 nm from 568 nm in THF. These feature changes are attributed to two effects; (1) the formation of molecular aggregates and (2) the change in environmental polarity upon increasing f_w.

In aggregated states, on one hand, the molecules take a closer packing mode, which may reduce the dihedral angle between the bridge and the adjacent phenyl in the TPE moiety. We carried out a calculation by setting the dihedral angle at 15°, and the result predicts a small energy gap (Fig. 3), corresponding to a red-shifted emission. On the other hand, the polar environment is facile to the photoinduced charge transfer (PICT) in the excited state, which helps the red-shift of the fluorescence spectrum for polar fluorogens. Increasing f_w is equivalent to enhancing the environmental polarity. As a result, the emission red-shifts accordingly. The slight emission enhancement at high f_w is due to the less polar local environment inside the molecular aggregates. Attachment of electron donor (D) groups onto the DPP core will enlarge the polarity and thereby enhance the PICT process, thus leading to further red-shifted emission. This will be validated and discussed below (Tables S1, S4 and S5, ESI†).

To further demonstrate the pivot role of the phenyl bridge, we attached two *N*,*N*-dimethylamine groups onto the two TPE moieties of **2**. Consequently, molecule **3** and its isomer **4** were derived. **3** and **4** exhibit similar properties despite that the *N*,*N*-dimethylamine groups have been attached to the phenyls on the opposite sides of the ethenyl of TPE moieties (Chart 1, Table S5, Fig. S15 to S18, ESI†). Herein, we use **3** as the representative. The absorption and emission peaks of **3** in THF solution appear at 500 and 564 nm, which are nearly identical to the data of **2** (496 and 568 nm, respectively, Tables S3 to S5, ESI†), though two strong electron donors have been introduced into the molecule. In addition, upon changing solvent polarity from hexane to *N*,*N*-dimethylformamide, the wavelengths of the absorption and emission peaks undergo a small red-shift (Fig. S15–S19, ESI†). Such a weak solvato-chromic effect is abnormal to the luminogens furnished with D and A groups.[11] A rational explanation is that the D–A effects of the two *N*,*N*-dimethyl-amines and DPP units are partially blocked by the phenyl bridges.

If the above deduction is trustworthy, the conformation between TPE and DPP units should be quite twisted thereby the twisted intramolecular charge transfer (ICT) should be observed. In apolar hexane solvent, **3** shows efficient emission (Φ_F = 59.6%, Table S4, ESI†); while in polar THF solvent, Φ_F drops to 0.2%. This is direct evidence of ICT, because the polar solvent is profitable to the ICT process,[11,12] which results in the non-irradiative decay. This Φ_F (0.2%) is much lower than that of DBr-Dph-DPP (95.2%) and **2** (43.8%) in THF solution. It can be attributed to the synergetic effect of the ICT process and the intramolecular rotations of phenyls on TPE moieties. Accordingly, the molecules could have higher fluorescent efficiency when they are in solid films. Indeed, the Φ_F of cast films is measured to be 8.6%, about 43 times higher than that recorded in THF solution, because the restricted intramolecular rotation (RIR) of phenyls has an effect and the lower polar environment in aggregates is disadvantageous to the ICT process.

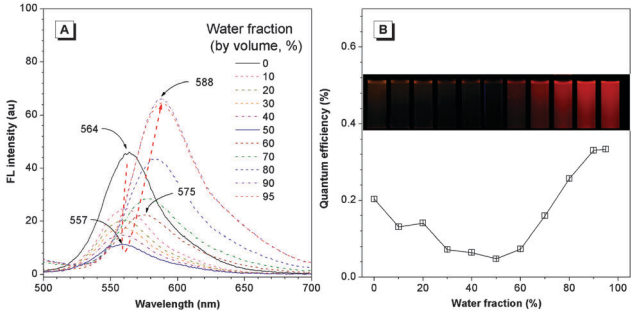

Fig. 4 Change in FL intensity (A) and quantum efficiency (B) of **3** in THF–water mixtures with different f_w values; the inset images show the corresponding FL photographs. Concentration: 10 μM; λ_{ex}: 365 nm.

We also monitored the fluorescent behaviors of **3** in THF–water mixtures with different f_w values (Fig. 4). When $f_w < 50\%$, the emission intensity monotonously decreases to negligible due to the ICT process. When $f_w \geq 50\%$, aggregates form in the system and the emission intensity boosts up due to the RIR and reduced ICT process. It is noticeable in Fig. 4A that the emission peak shows a blue-shift at lower f_w (0–50%, 564–557 nm) in solution and a red-shift at higher f_w (50–95%, 575–588 nm). The spectral shifts in the opposite directions imply that the molecules take a more or less twisted conformation in solvent mixtures and in aggregates, respectively.

The D–A structure bestows molecule **3** with strong dipole–dipole interaction, which may lead to the formation of ordered aggregates in mixture solvent. As shown in Fig. S20 (ESI†), at $f_w = 50\%$, ribbon-like structures of sizes of around 1 micrometer width and several tens to hundred micrometers length can be observed in the images of the scanning electron microscope (SEM). The red confocal fluorescent image is also displayed in Fig. S20 (ESI†). At higher f_w, the aggregates show a less ordered microstructure with smaller sizes. For DBr-Dph-DPP, **1** and **2**, no such well-ordered micro-structures can be observed under the same conditions (Fig. S21, ESI†). Also shown in Fig. S20 and S21 (ESI†) are the confocal fluorescent images of the aggregates of molecule **2** collected in the THF–water mixture with $f_w = 50\%$. The moderate fluorescence efficiency and red emission imply that their aggregates are useful candidates for bioimaging agents.

In summary, we have systematically investigated the fluorescent behaviors of the TPE–DPP conjugates by using rationally designed DPP derivatives, or molecules **1**, **2**, **3** and **4**. These molecules constructed by linking TPE (AIE-gen) and DPP (ACQ-gen) moieties with rotational phenyls demonstrate plentiful photo/electronic properties, including segmental electronic conjugation between the two building blocks, partially quenched fluorescence in solution, a limited solvatochromic effect in solvents with different polarity, a red-shifted emission band, and fractionally enhanced emission in the solid state. Together with the observation of the key role of the activation barrier in phenyl ring twisting on organic opto/electronics,[9,10] the present attempt, on one hand, disclosed instructive information about tuning the performance of organic luminogens by making subtle balance between AIE and ACQ units; and on the other hand, derived red-emitting molecules with good quantum efficiency and high stability.

This work was financially supported by the National Science Foundation of China (51273175) and the National Basic Research Program of China (973 Program, 2013CB834704).

Notes and references

1 (*a*) C. C. Wu, Y. T. Lin, K. T. Wong, R. T. Chen and Y. Y. Chien, *Adv. Mater.*, 2004, **16**, 61; (*b*) K. C. Wu, P. J. Ku, C. S. Lin, H. T. Shih, F. I. Wu, M. J. Huang, J. J. Lin, I. C. Chen and C. H. Cheng, *Adv. Funct. Mater.*, 2008, **18**, 67.
2 *Fluorescence Sensors and Biosensors*, ed. R. B. Thompson, CRC Press, LLC, Boca Raton, FL, 2006.
3 (*a*) J. Luo, Z. Xie, J. W. Y. Lam, L. Cheng, H. Chen, C. Qiu, H. S. Kwok, X. Zhan, Y. Liu, D. Zhu and B. Z. Tang, *Chem. Commun.*, 2001, 1740; (*b*) B. K. An, S. K. Kwon, S. D. Jung and S. Y. Park, *J. Am. Chem. Soc.*, 2002, **124**, 14410.
4 (*a*) Y. N. Hong, J. W. Y. Lam and B. Z. Tang, *Chem. Commun.*, 2009, 4332; (*b*) Y. N. Hong, J. W. Y. Lam and B. Z. Tang, *Chem. Soc. Rev.*, 2011, **40**, 5361.
5 Y. Dong, J. W. Y. Lam, A. Qin, J. Liu, Z. Li, B. Z. Tang, J. Sun and H. S. Kwok, *Appl. Phys. Lett.*, 2007, **91**, 11111.
6 (*a*) Q. Zhao, S. Zhang, Y. Liu, J. Mei, S. Chen, P. Lu, A. Qin, Y. Ma, J. Z. Sun and B. Z. Tang, *J. Mater. Chem.*, 2012, **22**, 7387; (*b*) Z. Zhao, S. Chen, J. W. Y. Lam, P. Lu, Y. Zhong, K. S. Wong, H. S. Kwok and B. Z. Tang, *Chem. Commun.*, 2010, **46**, 2221; (*c*) W. Z. Yuan, P. Lu, S. Chen, J. W. Y. Lam, Z. Wang, Y. Liu, H. S. Kowk, Y. Ma and B. Z. Tang, *Adv. Mater.*, 2010, **22**, 2159.
7 (*a*) S. Qu and H. Tian, *Chem. Commun.*, 2012, **48**, 3039; (*b*) Y. Qu, J. Hua and H. Tian, *Org. Lett.*, 2010, **12**, 3320; (*c*) M. M. Wienk, M. Turbiez, J. Gilot and R. A. J. Janssen, *Adv. Mater.*, 2008, **20**, 2556; (*d*) B. C. Thompson and J. M. J. Fréchet, *Angew. Chem., Int. Ed.*, 2008, **47**, 58.
8 (*a*) Q. Zhao, K. Li, S. Chen, A. Qin, D. Ding, S. Zhang, Y. Liu, B. Liu, J. Z. Sun and B. Z. Tang, *J. Mater. Chem.*, 2012, **22**, 15128; (*b*) Z. J. Zhao, P. Lu, J. W. Y. Lam, Z. M. Wang, C. Y. K. Chan, H. H. Y. Sung, I. D. Williams, Y. G. Ma and B. Z. Tang, *Chem. Sci.*, 2011, **2**, 672.
9 (*a*) M. A. Reed, C. Zhou, C. J. Muller, T. P. Burgin and J. M. Tour, *Science*, 1997, **278**, 252; (*b*) W. B. Davis, W. A. Svec, M. A. Ratner and M. R. Wasielewski, *Nature*, 1998, **396**, 60; (*c*) D. Segal, A. Nitzan, W. B. Davis, M. R. Wasielewski and M. A. Ratner, *J. Phys. Chem. B*, 2000, **104**, 3817.
10 (*a*) S. Ranganathan, I. Steidel, F. Anariba and R. L. McCreery, *Nano Lett.*, 2001, **1**, 491; (*b*) F. Anariba and R. L. McCreery, *J. Phys. Chem. B*, 2002, **106**, 10355; (*c*) F. Anariba, J. K. Steach and R. L. McCreery, *J. Phys. Chem. B*, 2005, **109**, 11163.
11 (*a*) X. Y. Shen, Y. J. Wang, E. Zhao, W. Z. Yuan, P. Lu, A. Qin, Y. Ma, J. Z. Sun and B. Z. Tang, *J. Phys. Chem. C*, 2013, **117**, 7334; (*b*) C. Reichardt, *Chem. Rev.*, 1994, **94**, 2319.
12 (*a*) X. Y. Shen, W. Z. Yuan, Y. Liu, Q. Zhao, P. Lu, Y. Ma, I. D. Williams, A. Qin, J. Z. Sun and B. Z. Tang, *J. Phys. Chem. C*, 2012, **116**, 10541; (*b*) J. Mei, J. Wang, A. Qin, H. Zhao, W. Z. Yuan, Z. Zhao, H. H. Y. Sung, C. Deng, S. Zhang, I. D. Williams, J. Z. Sun and B. Z. Tang, *J. Mater. Chem.*, 2012, **22**, 4290.

